Numerical Study of the Axial Impact of a Rigid Mass Against an Elastic Cantilever Beam

Amir Baharvand

1 Introduction

The axial impact of a rigid mass and an elastic cantilever beam is a classical problem. While the problem is discussed by several authors, the original solution is attributed to Saint-Venant. Todhunter, Isaac and Pearson [1], Graff [2] and Goldsmith [3] used the d'Alembert solution to wave equation together with the forward and backward wave equation to find the displacement field for different time intervals. Timoshenko and Goodier [4] used the equation of motion for various time increments. In the following, the analytical solution is not provided and only a brief introduction is presented.

The present report aims to provide a comparison between the analytical and numerical solution of the impact of a rigid mass and an elastic beam fixed at one end and is motivated by the previous work of Escalona *et.al.*[5]. This report is divided into two parts. The first part discusses the analytical solution and development of some basic mathematical equations. In the second part, ANSYS Explicit Dynamics and LS-DYNA are utilized for the numerical simulation of the problem.

2 Analytical Solution

2.1 Problem formulation

A schematic of the rigid mass and the elastic beam is depicted in Figure. 1. The mass has an initial velocity, v_0, and approaches the elastic beam in the positive direction of the x-axis while the elastic beam with a mass similar to the rigid body, m, Young's modulus, E, cross-sectional area, A, length, l is at rest. The beam is also fixed at the right end ($x = l$) and is free at x=0.

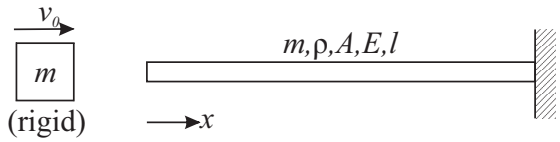

Figure 1: The problem geometry and coordinate system.

2.2 Assumptions

The following assumptions are made in developing the analytical solution.

1. The mass is assumed to be rigid and the beam is elastic.
2. The beam is long enough so that the one-dimensional wave equation is applicable.
3. At the time of impact, all the rigid body velocity is transferred to the beam.
4. The displacements are assumed to be infinitesimal.
5. No friction is assumed between the mass and beam. In addition, the contact is assumed to be perfect.
6. The effect of lateral inertia due to Poisson's ratio is disregarded. Furthermore, the vibration of the beam is neglected.

2.3 Discussion on the Analytical Solution

Due to the impact of the rigid mass with the elastic beam, a compressive stress wave, σ_0 is generated which propagates towards the positive x-direction. The third assumption states that after impact, the beam obtain the same velocity as the rigid mass that is

$$\sigma_0 = \rho c v_0 \tag{1}$$

where c is the wave propagation velocity. Due to the contact of two bodies, contact stress is generated, $\sigma(t)$, which can be calculated from the equation of motion.

$$m\frac{\mathrm{d}v(t)}{\mathrm{d}t} = -\sigma(t)A \tag{2}$$

The negative sign indicates compressive stress. One can correlate the stress and velocity via

$$\sigma(t) - \sigma(t_0) = \rho c[v(t) - v(t_0)] \tag{3}$$

where $\sigma(t_0)$ and $v(t_0)$ are the stress and velocity before the impact. Since the beam is at rest at t=0, the above equation reduces to $\sigma(t) = \rho c v(t)$. Replacing

$v(t)$ from the former line and m/A with M in combination with Eq. 2 results in the following differential equation.

$$\frac{M}{\rho c}\frac{\mathrm{d}\sigma(t)}{\mathrm{d}t} = -\sigma(t) \tag{4}$$

Solving Eq. 4 with the initial condition from Eq. 1 gives

$$\sigma(t) = \sigma_0 e^{-\frac{\rho c}{M}t} \tag{5}$$

which implies a decreasing behavior in the generated stress (see Figure. 2)

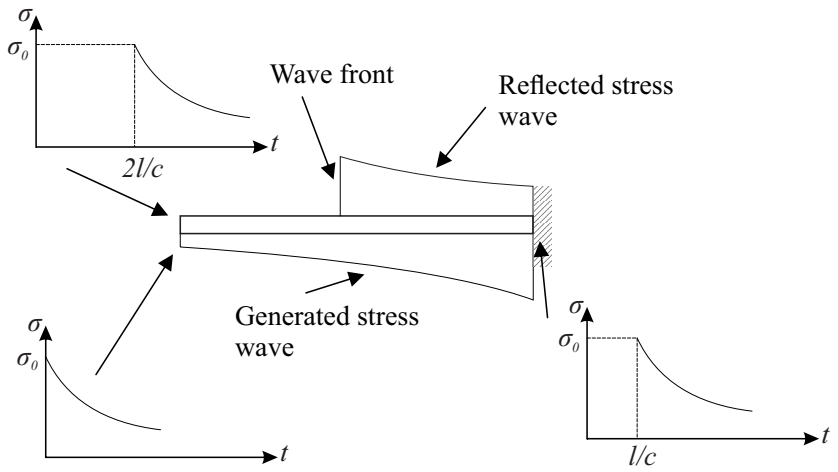

Figure 2: Illustration of the compressive stress waves (generated and reflected) during the first fundamental period.

Let T be the fundamental period that is the time required for the stress wave to travel through the beam and reflect ($T = 2l/c$). As soon as the stress wave arrives at the fixed boundary ($t = T/2$), it reflects as another compressive stress ($2\sigma_0$). At this instance, the contact stress can be calculated by setting $t = l/c$ in Eq. 5. At $t = T$, the total stress is increased by $2\sigma_0$. This jump in the total stress occurs for $nT, n = 2, 4, ...$ intervals; thus, enforcing to update the total stress equation at each fundamental period, T. After the first interval, the wave reflects as another compressive wave due to the existence of the rigid mass which resembles a fixed boundary. Consequently, the compressive wave is simply the generated wave from the previous time interval with a delay T. Finally, the total stress is the sum of the current stress and previous stress at $t = t - T$. Denoting the value of total stress at each interval by s

$$\sigma = s_n(t) + s_{n-1}(t - T) \tag{6}$$

The velocity is (see Eq. 3)

$$v = \frac{1}{\rho c}[s_n(t) - s_{n-1}(t-T)] \tag{7}$$

where n designates the intervals.

3 Numerical Analysis

3.1 Numerical Model

The mass and beam are modeled in ANSYS DesignModeler. The elastic beam material properties are listed in Table. 1 and the mass is modeled as a rigid body. The fixed boundary is applied at the end of the beam and the beam displacements are limited in the x and y directions (see Figure. 3). A frictionless contact is defined between two bodies and the solver is set to Lagrangian. The element type is linear as the solver does not allow to choose a quadratic element. An initial velocity of 1m/s is defined for the mass.

Table 1: Mechanical properties of the rigid mass and elastic beam.

Property	Symbol	Unit	Value	Attribution
Density	ρ	kg/m^2	7900	Mass/Beam
Length	l	m	0.3	Beam
Young's modulus	E	Pa	2.1E11	Beam
Poisson's ratio	ν	-	0.3	Beam
Mass	m	kg	2.133	Mass/Beam
Area	A	m^2	9E-04	Beam

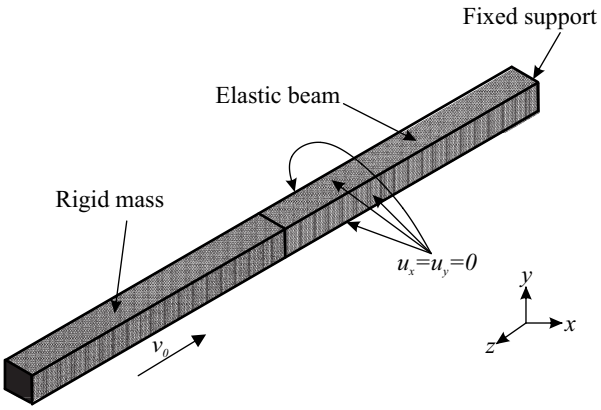

Figure 3: The numerical model.

3.2 Mesh Study

To achieve a robust numerical model, a mesh convergence study based on the area under the curve of stress-time from the initiation of contact to t=1.551E-05s is performed and compared to the theoretical value from Eq. 5. The absolute error is calculated from below.

$$\text{Error}[\%] = \frac{\sigma_1 - \sigma_2}{\sigma_2} \times 100 \tag{8}$$

where σ_1 and σ_2 denote the analytical and numerical values of stress, respectively. Table. 2 summarizes mesh number, N, size and the absolute error. The stress plots from the numerical method are given in Figure. 4a. Figure. 4b show that the mesh converges to below 1.5% for N=160000[1].

Table 2: Numerical model mesh information.

Number of elements (N)	Smallest dimension [m]	Absolute error[%]
160	0.0150	48.72
1280	0.0075	27.86
4320	0.0050	18.30
20000	0.0030	17.70
67500	0.0020	5.66
160000	0.0015	1.15

3.3 Results and Discussion

The displacement-time plot of the free-end of the elastic beam (x=0) is shown in Figure. 5. The numerical result follows the analytical solution curve until $T/2$; however, after this time, the difference between the two plots increases. It may seem that the reflected stress wave produces errors in calculating the displacement.

The stress distribution along the beam coordinate is plotted in Figure. 6 for three time cases (the first two, before $T/2$ and the last after $T/2$). These results are extracted from LS-DYNA as ANSYS Explicit Dynamics was not able to predict the falling behavior of the stress. Overall, the numerical model can predict the behavior of the stress distribution except for Figure. 6b. Due to the determination of stress from the displacement field in the finite element method (FEM) and good agreement between the analytical and numerical results in the displacement plot (Figure. 5), the author has no clear explanation for the stress plot in Figure. 6b. It is also evident from the plots that the number of mesh and time increment play a key role in the numerical result (see Figure. 6a and Figure. 6b) as the first value of stress at t=0 is almost half of the analytical

[1]Opting for a finer mesh less than the last row in Table. 2 causes the solver to crash due to limited RAM resources. Increasing the RAM in the `input.k` file and using the LS-Run and Mechanical APDL Product Launcher tools does not help.

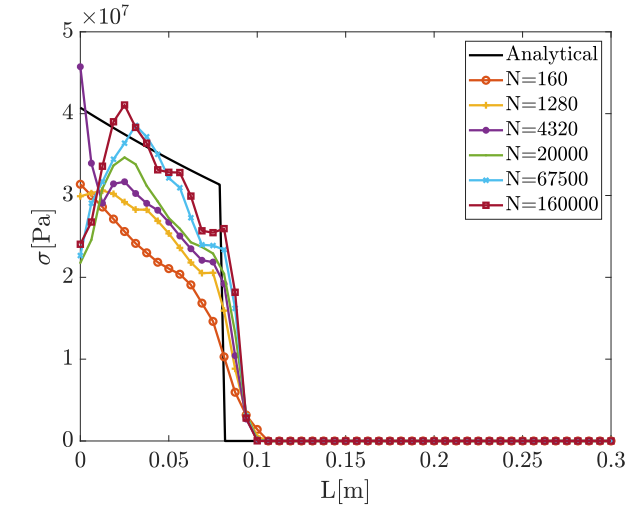

(a)

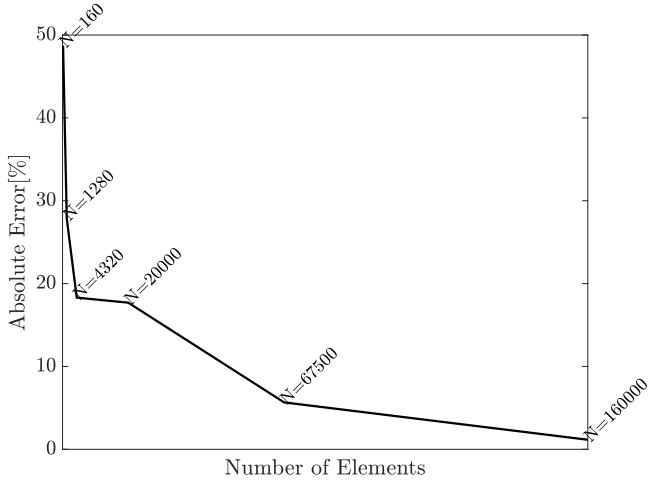

(b)

Figure 4: (a) Stress wave distribution along the beam coordinate at t=1.551E-05s for the different numbers of elements. (b) Mesh convergence plot.

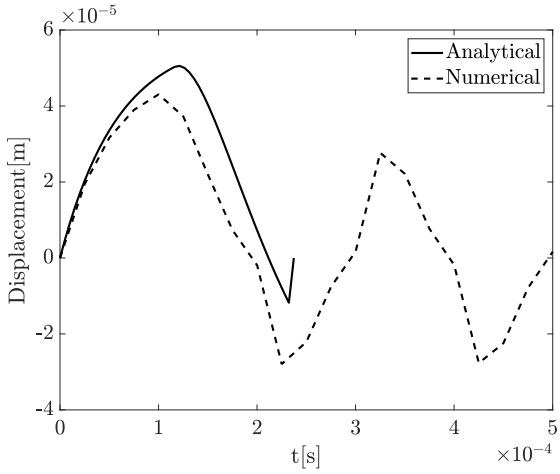

Figure 5: Displacement at the free-end of the beam (x=0) for various time increments ($t_{max} = T$).

solution then suddenly jumps to its corresponding analytical value.

Figure. 7 shows the distribution of contact pressure. Once more, the importance of a finer mesh is visible for the numerical result at t=0 and 1.25E-04s ($t = T$). At about $t = T$ the reflection of the stress wave from the rigid mass is obvious (see section 2.3).

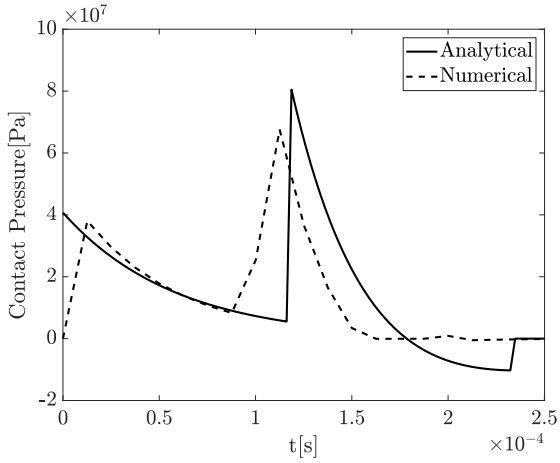

Figure 7: Contact pressure at the free-end of the beam (x=0) for various time increments ($t_{max} = 2T$).

The reaction stress (Figure. 8) is calculated from the reaction forces at the

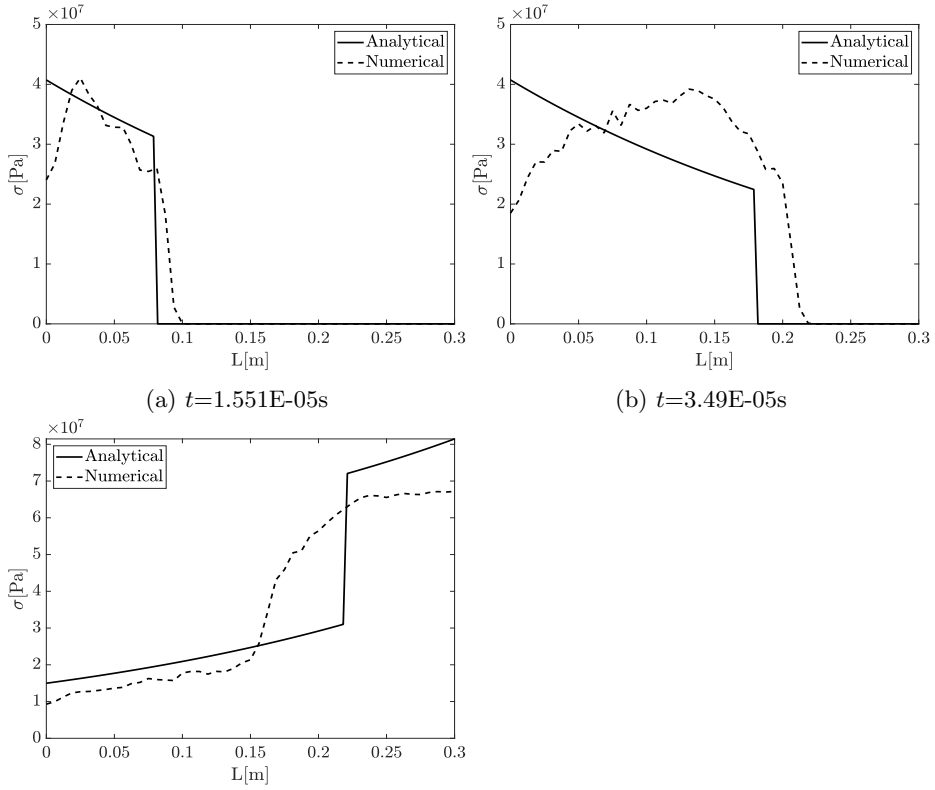

(a) t=1.551E-05s

(b) t=3.49E-05s

(c) t=7.370E-05s

Figure 6: Stress wave distribution along the beam coordinate for three time cases.

fixed boundary of the beam and then divided by the beam area. The numerical result shows a good agreement with the analytical until the end of the first period. The reaction stress is zero up to the arrival of the stress wave, generated at the free-end, then rises to $2\sigma_0$ due to the reflection of the stress wave. After $2T$, the numerical model fails to characterize the reaction stress due to the previously-mentioned reasons.

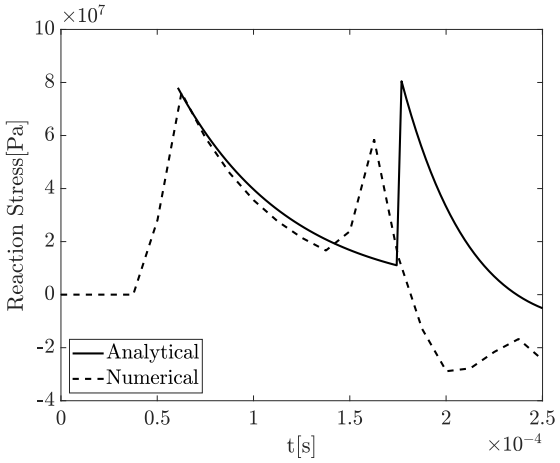

Figure 8: Reaction pressure at the fixed-support ($x = l$) for various time increments ($t_{max} = 2T$).

4 Conclusion

A brief introduction on the axial impact of a rigid mass against an elastic cantilever beam is provided. A numerical model is also developed and the results are compared to the analytical model. It is shown that the numerical model underestimates the displacement and stress which can be a result of the limited degrees of freedom in the finite element method (FEM). FEM is incapable of predicting the correct displacement of a multi degree-of-freedom system as the degrees of freedom in a numerical model is limited. In addition, the importance of the mesh convergence study with a fine mesh at the contact surfaces along with smaller time increments is emphasized.

References

[1] I. Todhunter and K. Pearson, *A History of the Theory of Elasticity and of the Strength of Materials*. C. J. Clay, M.A and Sons at University Press, part ii saint-venant to lord kelvin ed., 1893.

[2] K. F. Graff, *Wave Motion in Elastic Solids*. Dover Publications, New York, 1975.

[3] W. Goldsmith, *Impact: the Theory and Physical Behaviour of Colliding Solids*. Dover Publications, 2001.

[4] S. Timoshenko and J. N. Goodier, *Theory of Elasticity*. New York: McGraw-Hill, third ed., 1970.

[5] J. L. Escalona, J. Mayo, and J. Domínguez, "New numerical method for the dynamic analysis of impact loads in flexible beams," *Mechanism and Machine Theory*, vol. 34, no. 5, pp. 765–780, 1999.